



HAL
open science

Design and test of an open portable MRI system

Simon Chauvière, Lamia Belguerras, Thierry Lubin, Smail Mezani

► **To cite this version:**

Simon Chauvière, Lamia Belguerras, Thierry Lubin, Smail Mezani. Design and test of an open portable MRI system. *COMPEL: The International Journal for Computation and Mathematics in Electrical and Electronic Engineering*, 2022, 41 (4), pp.1084-1095. 10.1108/COMPEL-11-2021-0436 . hal-03626840

HAL Id: hal-03626840

<https://hal.science/hal-03626840>

Submitted on 31 Mar 2022

HAL is a multi-disciplinary open access archive for the deposit and dissemination of scientific research documents, whether they are published or not. The documents may come from teaching and research institutions in France or abroad, or from public or private research centers.

L'archive ouverte pluridisciplinaire **HAL**, est destinée au dépôt et à la diffusion de documents scientifiques de niveau recherche, publiés ou non, émanant des établissements d'enseignement et de recherche français ou étrangers, des laboratoires publics ou privés.

Design and test of an Open Portable MRI System

Simon Chauvière, Lamia Belguerras, Thierry Lubin, Smaïl Mezani
Université de Lorraine, GREEN, Nancy, France

Abstract—

Purpose: The purpose of this paper is the design study and realization of portable low-field open MRI system..

Design/Methodology/Approach: In this work, a design study and realization of Portable Low-Field open MRI System is proposed. The design of the MRI system is based on an optimization study using a genetic algorithm. Non-linear 2D and 3D numerical electromagnetic models are developed and inserted in the optimization environment.

Findings: The results are found to be consistent with those issued from fully experimental tests. The static field produced by the device is 0.295 T with a homogeneity of 2.8 % (28000 ppm) over 100 mm Diameter Sphere Volume (DSV). The z-axis gradient coils are capable of generating switching gradients with amplitude of 8 mT/m and frequency of 1.2 kHz.

Originality/Value: Our system is an open portable MRI which can be used in an ambulance. The open topology permits an easy access into the lateral sides when a surgery using surgical instrument with video feedback is needed.

Keywords—MRI, design, finite elements, modelling, permanent magnets, optimization

I. INTRODUCTION

MRIs are increasingly used in medical diagnosis and surgery thus requiring the installation of a large number of scanners. However, access to MRI scanners is limited by systems installations and post-installation maintenance cost, complexity of operating an MR system and infrastructure requirements. Hence, large patient populations are deprived from access to MRI, in particular for patients who cannot be transported safely to the scanner or who are in low-resource environments. In recent years, the design of MRI systems with field strengths significantly lower than those at 1.5 T and 3 T has known an interest for use in standard clinical examinations [1]– [3]. In literature, it has been shown that there is a significant reduction in signal-to-noise ratio (SNR) at low fields and there is fewer patient contraindications [4].

There are several commercial low field MRI systems having a single ferromagnetic yoke (C shape) or two ferromagnetic yokes (H shape) to close the flux with B_0 intensity between 0.1 and 1 T. To create B_0 , two large discs of permanent magnets (PMs) are placed above and below the gap in which the patient is positioned. These systems are heavy (over 1000 kg) [5]. Recently, reduced size and cheap MRI scanner with $B_0 = 60$ mT has been developed for emergency applications [6]. Its weight of about 500 kg which limits its transportability.

Low-field extremity MRI scanners are specifically used for imaging leg, hand, arm, or foot [7]. They are useful to diagnose problems with muscles, bones, joints, nerves or blood vessels. These systems are heavy, for example, a commercial 1 T hand / wrist imager can be installed in an area requiring a floor that can support nearly 2000 kg [2]. The most common geometry of extremity MRI systems is a discretized version of a Halbach magnets, which produces the highest homogeneous magnetic field inside a tunnel [8], [9]. However, even if they are transportable, the intensity of B_0 is less than 0.1 T and the iron bore of this type of systems is open only along the cylinder. So, it doesn't permit access into the lateral sides to allow, for example, the use of surgical instruments.

In this paper, we propose the design and test of an open low- cost extremity portable and lightweight MRI system. The originality of the proposed MRI system is that the Permanent Magnets discs are placed between two pole pieces having cylindrical and crown shapes respectively. This design improves the homogeneity of B_0 compared to the topology in which the PM disc is placed between an iron yoke and a cylindrical pole piece [10], [11]. Furthermore, the iron yoke used to close the magnetic flux is open within four sides (fig. 1). This allows an easy access to the imaging zone along a DSV of 10 cm and may constitute a good alternative to the commercialized cylindrical systems cited above.

The proposed low- field MRI system is composed of rare-earth discs PMs to generate a static magnetic field B_0 of 0.3 T. In addition, two solenoids are wound around the magnets to produce a switching gradient field intensity of 8 mT/m with a frequency of 1.2 kHz. In addition, the proposed system is compact since its dimensions are (35x35x30) cm and its weight is only 120 kg. Indeed, it can be transportable aboard a car or an ambulance.

The design of the proposed MRI uses genetic algorithms to optimize the structure, the objectives are to maximize the homogeneity of B_0 and the linearity of z-axis gradient field G_z .

In order to reduce the CPU time during the optimization procedure, the iron yoke of the proposed structure is simplified to a cylindrical shape. In this case, a non-linear axisymmetric two-dimensional (2D) finite elements model has been developed to compute the static magnetic field distribution and the gradient magnetic field. Then, the model has been inserted in the optimization procedure.

The cylindrical iron yoke of the optimal structure has been changed with an open one composed of a base and top parts separated by four pillars. For this structure, a three-dimensional (3D) finite elements computation permitted to check the measured values of B_0 and G_z .

II. DESCRIPTION OF THE STUDIED MRI SYSTEM

The main components of the system are the permanent magnets and z-axis gradient coils module. The overall layout of the components of the studied system is shown in Fig. 2. It is composed of an open iron yoke with two axially magnetized disc magnets facing each other and separated by an air region containing the Diameter Sphere Volume (DSV). Each magnet is located between an iron disc and a crown shaped iron disc. The crown shape of the iron disc is chosen to improve the homogeneity of B_0 . The z-axis gradient coils module is composed of two coils. Each one is mounted around a permanent magnet disc. The geometry of the structure is open as to allow easy access to the homogeneity zone.

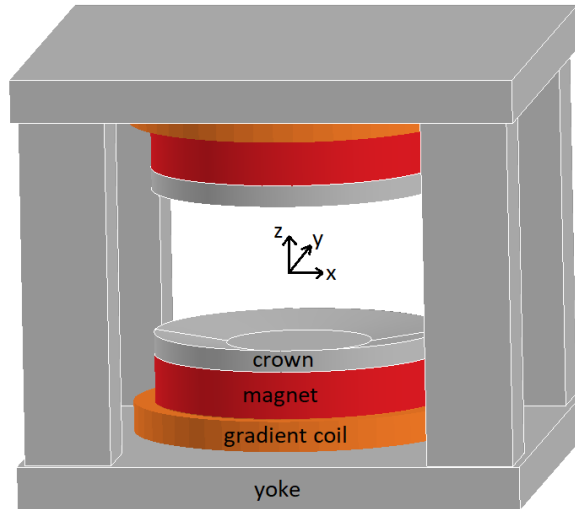


Fig. 1 Three-dimensional representation of the studied MRI system

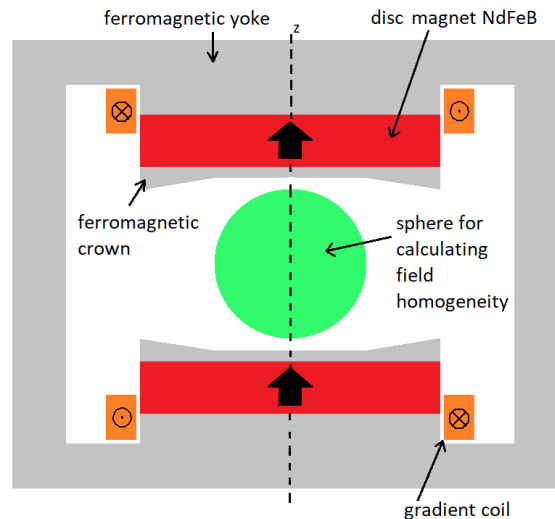


Fig. 2 Two-dimensional representation of the studied MRI system

III. DESIGN AND OPTIMIZATION OF THE STRUCTURE

To design the studied MRI system, two steps are needed: The first step consists of simplifying the open iron yoke geometry into a cylindrical one to have a circular symmetry around the z-axis (Fig. 2). The goal is to reduce the time consuming of the optimization procedure. For this structure, a numerical 2D-Axisymmetric model based on Finite Elements Method (FEM) computation is developed by using FEMM software [12]. Then, the model is inserted into an optimization environment using

genetic algorithms. In the second step, the iron yoke of the obtained optimal structure is replaced by an open one (Fig. 1), it consists of two parts; the base and the top: separated by four ferromagnetic pillars. In order to verify the results of the 2D analyses (B_0 distribution and its homogeneity in the DSV), 3D finite element computations are performed by using Flux-3D software.

Rare earth magnets (Neodymium-Iron-Boron) with high remanent flux density ($B_r = 1.3$ T) are used. The crown shape of the ferromagnetic discs improves significantly the B_0 homogeneity in the useful area [13], [14]. The optimization performed in this study uses a single objective genetic algorithm (GA). It has been shown that it provides potential solutions with high diversity for non-linear optimization of MRI systems [15], [16]. In this paper, the static magnetic field B_0 and the gradient field linearity along z-axis (G_z) are the objectives of the optimization process. So, it needs multi-objectives optimization algorithm. Since the multi-objectives optimization computation using a numerical model takes long time, we opted for mono-objective optimization of B_0 homogeneity and the gradient magnetic field (G_z) linearity separately.

First, the system without gradient coils is considered to maximize the B_0 homogeneity. Then, the gradient coils are added to the obtained optimal geometry to optimize G_z linearity.

A. B_0 optimization

The geometrical parameters of our structure are shown in Fig. 3. The radius of the disc magnets is $R_{\text{magnet}} = 10$ cm and its height is $H_{\text{magnet}} = 3.5$ cm. The distance between the center of the structure and the iron crown is set to 5 cm to leave sufficient space in the center. The range of variation of the others parameters is given in Table I.

For the 2D finite element simulations, the axisymmetric geometry shown in Fig. 2 has been replaced by the simplified one shown in Fig. 3 which considers the symmetries of the problem. FEMM software [12] uses a Magnetic Vector Potential formulation (noted A) to solve this 2D magnetostatics problem. At $r = 0$, the flux lines are parallels to the boundary and a Dirichlet boundary condition has been specified ($A = 0$). At $z = 0$, the flux lines are perpendicular to the boundary and a Neumann boundary condition has been specified ($\partial A / \partial n = 0$). In order to simplify the study and reduce the computation time of the optimization procedure, all the boundaries that correspond to the ferromagnetic yoke has been replaced by a perfect magnetic boundary condition (the flux line are perpendicular to these boundaries, $\partial A / \partial n = 0$). This assumption is correct because all the yoke dimensions have been chosen to work under the knee point of the $B(H)$ curve of the used ferromagnetic material.

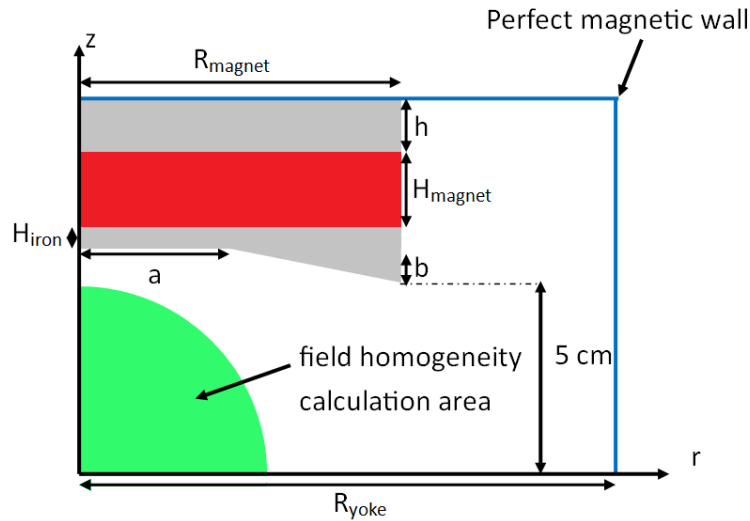


Fig. 3 Axisymmetric (2D) model and definition of the geometric parameters

TABLE I. VARIATION RANGES OF THE PARAMETERS

Parameters	Min values (cm)	Max values (cm)
R_{yoke}	10	15
H_{iron}	0.3	1
a	0.1	9.9
b	0	1
h	0.5	5

The parameters of the optimal structure are determined by carrying out a single-objective optimization under constraints with a genetic algorithm available in Matlab. The objective function is the increase the homogeneity of the magnetic field in a sphere with a radius of 5 cm. This is achieved by minimizing the following function:

$$F_S = (B_{\max} - B_{\min}) / B_0$$

where B_{\max} and B_{\min} are the maximum and minimum values of z-axis static magnetic flux density in a DSV of 5 cm and B_0 is the value of the flux density at the center.

The parameters resulting from the optimization are presented in Table II. For these parameters, a static magnetic field of 0.301 T is obtained at the center while the homogeneity in the DSV zone is about 1.63 %. Fig. 4 shows the distribution the static magnetic field magnitude in the homogeneity area.

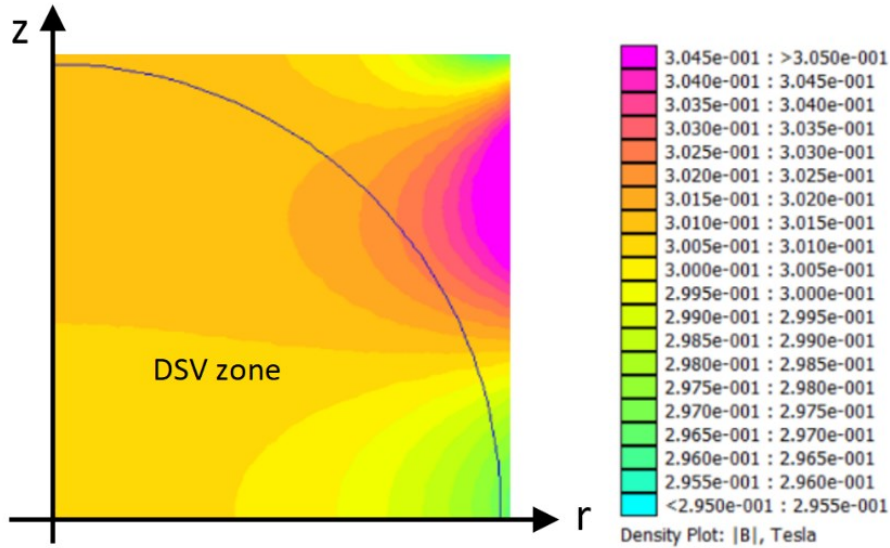


Fig. 4 Map of the magnetic field B_0 in the plane (rz)

TABLE II. PARAMETERS RESULTING FROM THE OPTIMIZATION

Parameters	Values (cm)
R_{yoke}	15
H_{iron}	0.7
a	5
b	0.8
h	2

B. Optimization of gradient coils

In order to generate a gradient field along the z-axis two coils are used around the permanent magnets (as shown in Fig. 2) and supplied with the same direct-current (DC) current but in opposite direction.

The optimal structure obtained previously will not be modified for the optimization of the gradient coils. The parameters to be optimized (Fig. 5) are only the dimensions of the coils, such as h_{coil} and e_{coil} , the position of the coils (R_{intcoil} and L) and the total current in the coils (I_{coil}). The range of variation of these parameters is given in Table III.

The magnetic equations solved by FEMM are the same as in the previous section (magnetostatics problem, magnetic vector potential formulation). The boundary conditions are also the same at $r = 0$ and for the ferromagnetic yoke limiting surfaces. The only difference is the boundary condition at $z = 0$ where the flux line distribution are now parallels to this boundary. Thus, a Dirichlet boundary condition is specified ($A=0$).

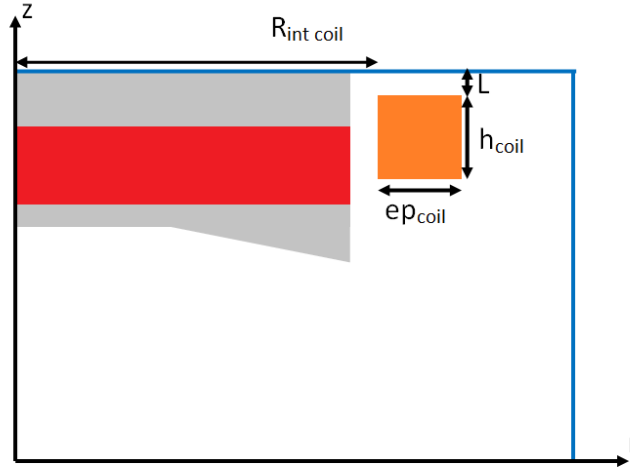


Fig. 5 Definition of the geometrical parameters of the gradient coils

TABLE III. VARIATION RANGES OF THE PARAMETERS

Parameters	Min values (cm)	Max values (cm)
$R_{intcoil}$	10.1 cm	14 cm
L	0.1 cm	5 cm
ep_{coil}	0.1 cm	5 cm
h_{coil}	0.1 cm	5 cm
I_{coil}	0 A	300 A

These parameters are determined by performing a single-objective optimization under constraints. These parameters will be constrained by either the geometry of the structure and by the maximum value of the current density in the coils set at 2 A/mm² to avoid heating effect. This optimization is again performed using the same genetic algorithm used above. The static and gradient field amplitudes have several orders of magnitude of difference (0.3 T versus less than 1 mT).

In order to be able to discern the gradient field, the remanent field of the magnets is set to zero in the FEMM simulation so only the magnetic field created by the gradient coils will be considered. In so doing, the contribution of the PM magnetic field is ignored which results in a wrong permeability distribution in the saturated iron parts. A simple solution to overcome this problem is to compute the field distribution due to PMs (non-linear FEM) and freeze the magnetic permeability distribution to compute the gradient field due to the coil's currents alone. The "Frozen Permeability" feature available in FEMM software allows this type of computation. This kind of computation significantly increases the computation time and is not suitable for an optimization procedure. Therefore the "Frozen Permeability" method will not be used in the gradient coils optimization but will be used afterward for frequency-domain computations intended to check the measurements.

The desired gradient field is given by $B_{z,desired} = G_z z$ along the z-axis where $G_z = 8$ mT/m. In order to have a gradient field as close as possible to the desired one, we choose to minimize the following criteria:

$$F_G = \sum_i (B_{g,desired,i} - B_{g,i})^2$$

where $B_{g,desired,i}$ and $B_{g,i}$ are values of the flux density along the z-axis ($0 < z < 5$ cm).

The parameters resulting from the optimization are given in Table IV. Fig. 6 shows the obtained gradient field plot along the z-axis with the desired gradient field. A gradient field of 8 mT/m is obtained; however, it is difficult to obtain a linear variation of the flux density along the z-axis meeting the specifications over such a large length (5 cm). The presence of the iron crowns, which favor the homogeneity of the static field, does not allow the desired gradient field to be obtained.

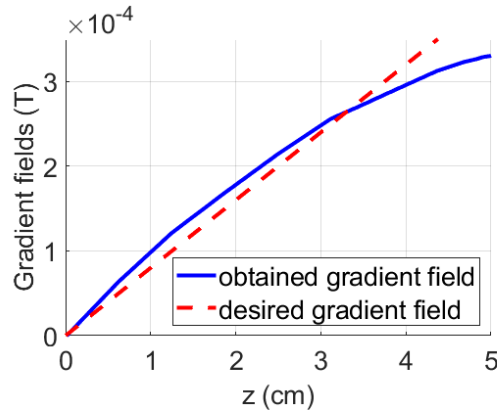


Fig. 6 Gradient fields along the z-axis

TABLE IV. PARAMETERS RESULTING FROM THE OPTIMISATION

Parameters	Values (cm)
R_{intcoil}	10.1 cm
L	0.2 cm
e_{pcoil}	1.4 cm
h_{coil}	2.1 cm
I_{coil}	167 A

IV. BEHAVIOR OF THE STRUCTURE WHEN SUPPLIED WITH ALTERNATING CURRENT

In an MRI, the gradient coils are used, among other things, to define the slice plane of the image to be obtained. They are therefore fed in a precise sequence with trapezoidal time-varying currents. The aim of this part is to study the response of our device when the gradient coils are supplied with an Alternating Current (AC).

The gradient coils generate a high frequency magnetic field. This field variation induces eddy currents in the solid conductive parts (magnets and iron) which can affect the gradient field [17]. In addition, these eddy currents can also result in heat generation in the magnets and the iron. The effect of varying the gradient coils frequency is studied in sinusoidal regime with a 2D axisymmetric magneto-harmonic model using the ‘‘Frozen Permeability’’ method of FEMM.

Fig. 7 shows the gradient field along the z-axis for different frequencies. For all the frequencies, the current in the coil is maintained constant and equal to 167A. The finite element simulation shows that the field gradient decreases as the frequency increases. This is due to the effect of the induced currents in the conductive parts (magnets and iron). These induced-currents generate a reaction magnetic field opposite to the one obtained by the gradient coils. As the frequency increases, the obtained gradient field deviates from the desired gradient field. For a frequency of 1000 Hz, Fig. 7 shows that the gradient field magnitude is only of 1.3 mT/m instead of 8 mT/m. For this frequency, it would be necessary to increase the current in the gradient coils from 167A to 550A to maintain the gradient field magnitude to its rated value. However, this will have a significant impact on the Joule losses in the coils and will cause an increase in temperature inside the MRI with a risk of magnets demagnetization.

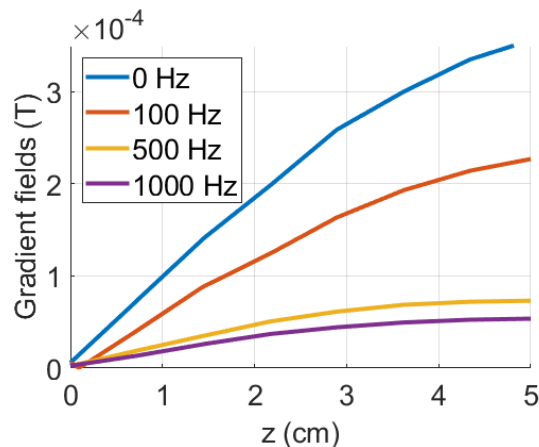


Fig. 7 Gradient fields along the z-axis for different frequency, obtained with FEMM

V. EXPERIMENTAL VALIDATION

The MRI prototype has been constructed by ECS France Magnet Engineering [18]. A photo of the prototype is shown on Fig. 8.

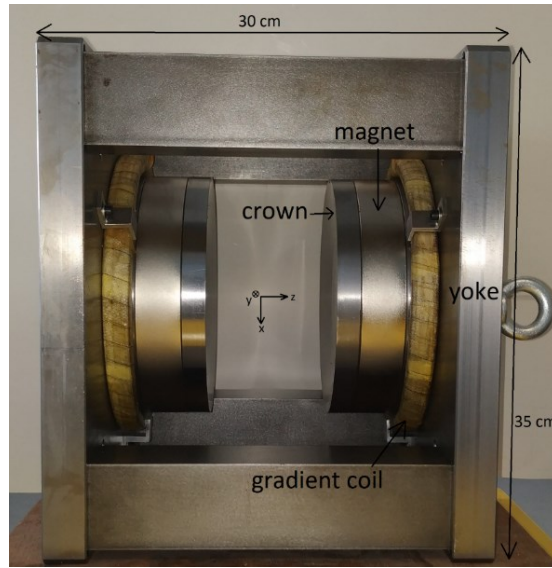


Fig. 8 Picture of the MRI system

A. Static field validation

The measurements of the static magnetic field were performed with a GM08 Hall Effect probe from Hirst Magnetic Instrument Ltd. The magnetic field in the plane (xz) at $y = 0$ can be seen on Fig. 9. The calculation of homogeneity gives us a value of 2.8 % (28000 ppm) on a sphere of 5 cm radius for a static field of 0.295 T at the center, which is very close to value obtained from the 3D simulation which was 2.6 % for a field of 0.302 T. This result shows the quality of the realization of the prototype for the small MRI.

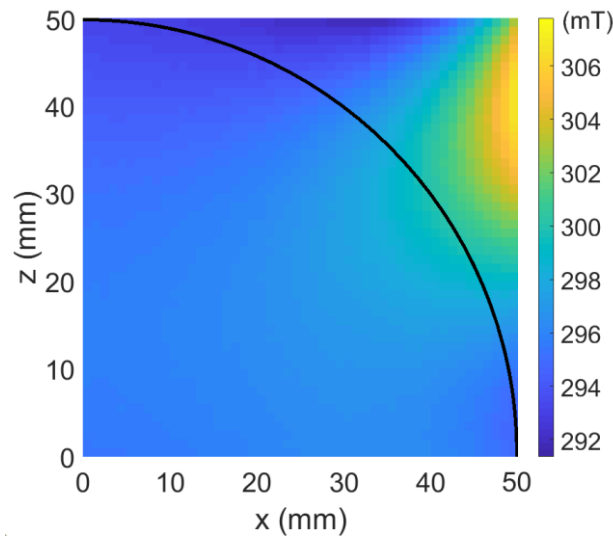


Fig. 9 Map of the magnetic field B_0 in the plane (xz) at $y=0$

B. Gradient field validation

The measurements of the gradient field were performed at different frequencies. For a static gradient field (at $f = 0$ Hz), the gradient field is obtained by first measuring the magnetic field with no current in the gradient coil and then measuring it with a current in the gradient coils, the difference between those two measurements gives the gradient field. Fig. 10 shows the gradient field along the z -axis with a linear regression of the measurement point, the gradient field is calculated with Flux-3D software and with FEMM ("Frozen Permeability" method).

For the 3D problem that corresponds to the actual geometry of our system (Fig. 1), we have used the Flux-3D software to compute the gradient field distribution obtained in Fig. 10 (static field). To solve this problem, Flux-3D software uses a reduced magnetic scalar potential formulation with respect to H_j which is defined by $H = -\nabla\phi + H_j$ for the regions with electrical current (coils). By using this method, the magnetic field created by the coils is analytically calculated (non-meshed coils). The boundary conditions are imposed on the surfaces of an infinity box (ten times the size of our system) where the magnetic potential is set to 0 ($\phi=0$).

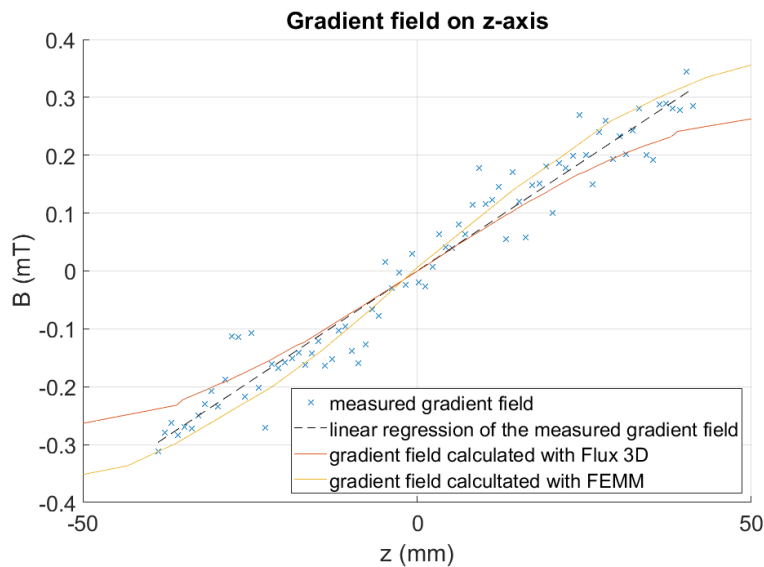


Fig. 10 Gradient field along the z-axis for $f = 0$ Hz

It can be seen in Fig.10 that the results obtained with Flux-3D are slightly lower than the measured values while the FEMM results are slightly higher. The FEMM simulation is a 2D axisymmetric model while the actual ferromagnetic parts which close the magnetic flux are not cylindrical (see Fig. 1, pillars and yoke). Thus, the flux lines path is shorter for the 2D model which imply a lower magnetic resistance resulting in a higher flux density obtained with this 2D model compared to the measurements. The Flux-3D simulations does not use the Frozen Permeability method like the FEMM simulation, only the magnetic field created by the coils is considered and not the magnetic field created by the magnets (otherwise the magnetic field of the coils is not discernable from the magnetic field generated by the magnets, the ratio is around 1000). The magnetic state of the ferromagnetic crown in this simulation is therefore different from the real one which is saturated. Thus, the magnetic field in this simulation is lower than the measured ones.

The measurements of the gradient field at non-null frequency were performed with a three-axis Hall Magnetometer from Metrolab, the value of the gradient field is measured on the z-axis at 4.6 cm of the center of the DSV. The attenuation of the gradient field with the frequency can be seen in Fig. 11. The measured gradient field is close to the one calculated with the simulation. Therefore, it is possible to predict the attenuation of the gradient field due to the frequency and thus to estimate the right current value which allows to maintain the gradient field at its desired value.

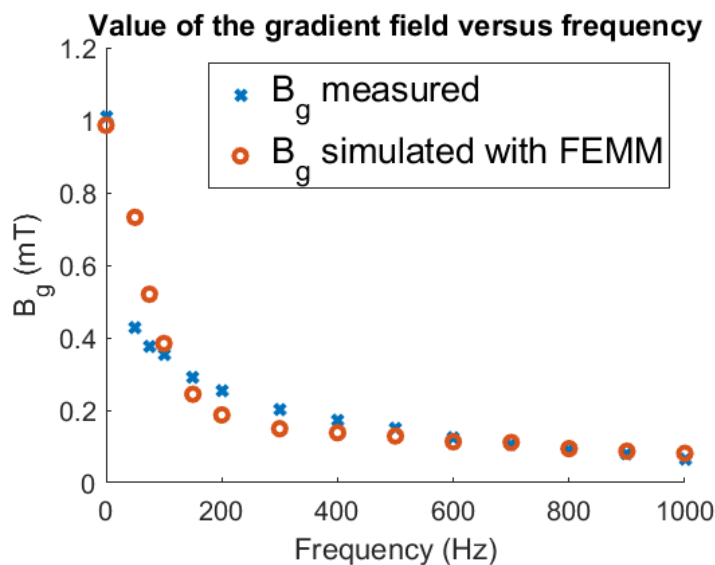


Fig. 11 Value of the gradient field versus frequency for the finite element (FEM) simulation and the experimental measurement. These measurements are taken on the z-axis at 4.6 cm of the center of the DSV

VI. CONCLUSION

In this work, we have presented the design, construction and tests of a low-field open portable MRI system allowing easy access to the homogeneous field zone. Our structure is composed of permanent magnets to create a B_0 of 0.3 T and z-axis gradient coils to generate a field gradient of 8 mT/m. In order to reduce the CPU time during the optimization procedure to design the studied structure, the iron yoke is simplified to a cylindrical shape. Then a non-linear 2D finite element model has been developed to compute the static magnetic field distribution and the gradient magnetic field in the homogeneity zone. This model has been integrated into genetic optimization algorithms. A non-linear 3D finite element model of the optimal structure with an open iron yoke has been developed to check the homogeneity of B_0 and the linearity of G_z . The results are found to be consistent with the measurements. The multi-turns z-axis gradient coils were optimized for gradient strength and linearity using 2D FEM computations. The proposed configuration uses permanent magnets to generate a static magnetic field of 0.295 T with a measured homogeneity of 2.8 % (28000 ppm) over 100 mm DSV. The coils wound around the magnets allowed a gradient field $G_z = 8$ mT/m at low frequencies but the presence of the solid iron pieces caused an attenuation of G_z when the frequency increases. However, it is possible to measure and simulate this attenuation and therefore to increase the current in the gradient coils in order to maintain the desired gradient field magnitude. The proposed MRI system is compact since its dimensions are (35x35x30) cm and its weight is only 120 kg which makes it transportable aboard a car or an ambulance. This MRI system will be completed by x and y-axis gradient coils. In order to keep the access to the imaging zone, the diameter of those coils should be greater than 10 cm.

ACKNOWLEDGEMENTS

The authors would like to acknowledge the Institut Carnot ICEEL, Nancy, France, for the financial support of this work.

REFERENCES

- [1] Tsai LL, Mair RW, Rosen MS, Patz S, Walsworth RL. An openaccess, very-low-field MRI system for posture-dependent He-3 human lung imaging. *J Magn Reson.* 2008;193:274-285. 5.
- [2] Macovski A, Conolly S. Novel approaches to low-cost MRI. *Magn Reson Med.* 1993;30:221-230.
- [3] E. Chiricozzi, C. Masciovecchio, M. Villani, A. Sotgiu and L. Testa, "Multipolar laminated electromagnet for low-field magnetic resonance imaging and electron paramagnetic resonance imaging," in *IEEE Transactions on Biomedical Engineering*, vol. 45, no. 7, pp. 928-933, July 1998, doi: 10.1109/10.686801.
- [4] Marques JP, Simonis FFJ, Webb AG. Low-field MRI: An MR physics perspective. *J Magn Reson Imaging.* 2019;49(6):1528-1542.
- [5] Sarracanie M, LaPierre CD, Salameh N, Waddington DEJ, Witzel T, Rosen MS. Low-cost high-performance MRI. *Sci Rep.* 2015;5:15177.
- [6] Kevin Sheth, Bradley Cahn, Sadegh Salehi, et al. "First Deployment of a Portable, Bedside, Low-Field Magnetic Resonance Imaging Solution for Artificial Intelligence Based Application (2771)", *Neurology*, April 14, 2020.
- [7] Sutter R, Tresch F, Buck FM, Pfirrmann CW. Is dedicated extremity 1.5-T MRI equivalent to standard large-bore 1.5-T MRI for foot and knee examinations?. *AJR Am J Roentgenol.* 2014;203(6):1293-1302.
- [8] O'Reilly T, Teeuwisse WM, de Gans D, Koolstra K, Webb AG. In vivo 3D brain and extremity MRI at 50 mT using a permanent magnet Halbach array. *Magn Reson Med.* 2021;85
- [9] Cooley CZ, McDaniel PC, Stockmann JP, et al. A portable scanner for magnetic resonance imaging of the brain [published online ahead of print, 2020 Nov 23]. *Nat Biomed Eng.* 2020;10.1038/s41551-020-00641-5.
- [10] Sahebjavaher, R. S., Walus, K., & Stoerber, B. Permanent magnet desktop magnetic resonance imaging system with microfabricated multiturn gradient coils for microflow imaging in capillary tubes. *The Review of scientific instruments*, 81(2), 023706, 2010.
- [11] Wright, S.M., Brown, D.G., Porter, J.R. et al. A desktop magnetic resonance imaging system. *MAGMA* 13, 177–185 (2001).
- [12] D. C. MEEKER, Finite Element Method Magnetics Version 4.2 (1 October 2011 Build) <http://www.femm.info>
- [13] Raoult, G., Adamski, J., Cueille, J. P., Laval, C., & Roux, R. (1962). Obtention de champs magnétiques homogènes. *Journal de Physique Appliquée*, 23(S3), 47-51
- [14] Nguyen, V. (1996). *Système de création de champ magnétique homogène à aimants ferrites pour l'imagerie RMN* (Doctoral dissertation, Institut Polytechnique de Grenoble)
- [15] Cooley, C. Z., Haskell, M. W., Cauley, S. F., Sappo, C., Lapierre, C. D., Ha, C. G., ... & Wald, L. L. (2017). Design of sparse Halbach magnet arrays for portable MRI using a genetic algorithm. *IEEE transactions on magnetics*, 54(1), 1-12
- [16] Yao, Y., Fang, Y., Koh, C. S., & Ni, G. (2005). A new design method for completely open architecture permanent magnet for MRI. *IEEE Transactions on Magnetics*, 41(5), 1504-1507
- [17] Xu, Z., Wu, J., Li, L., He, Y., He, W. and Yu, D. (2017), "Fast analytical calculation method for eddy current induced by gradient fields in an MRI system", *COMPEL - The international journal for computation and mathematics in electrical and electronic engineering*, Vol. 36 No. 6, pp. 1690-1705
- [18] ECS France Magnet Engineering, <http://www.ecs-global.fr>